frontiers | Frontiers in Earth Science

TYPE Original Research
PUBLISHED 19 January 2023
DOI 10.3389/feart.2022.1078624

Check for updates

OPEN ACCESS

EDITED BY
Fanyu Zhang,
Lanzhou University, China

REVIEWED BY
Kun Fang,
China University of Geosciences Wuhan, China
Armstrong Ighodalo Omoregie,
University of Technology Malaysia, Malaysia

*CORRESPONDENCE
Penghui Li,
2015995276@qq.com

SPECIALTY SECTION
This article was submitted to Geohazards and Georisks, a section of the journal Frontiers in Earth Science

RECEIVED 24 October 2022
ACCEPTED 28 November 2022
PUBLISHED 19 January 2023

CITATION
Yang H, Li P, Yang E, Jiang X and Chen J (2023), The strength law of coir fiber-reinforced soil based on modified Duncan-Chang model.
Front. Earth Sci. 10:1078624.
doi: 10.3389/feart.2022.1078624

COPYRIGHT
© 2023 Yang, Li, Yang, Jiang and Chen. This is an open-access article distributed under the terms of the Creative Commons Attribution License (CC BY). The use, distribution or reproduction in other forums is permitted, provided the original author(s) and the copyright owner(s) are credited and that the original publication in this journal is cited, in accordance with accepted academic practice. No use, distribution or reproduction is permitted which does not comply with these terms.

The strength law of coir fiber-reinforced soil based on modified Duncan-Chang model

Hui Yang[1,2], Penghui Li[2]*, E Yang[1], Xueliang Jiang[1,2] and Jiayu Chen[2]

[1]School of Civil Engineering and Engineering Management, Guangzhou Maritime University, Guangzhou, China, [2]School of Civil Engineering, Central South University of Forestry and Technology, Changsha, China

A large diameter triaxial sample of 61.9 mm was made by adding coir fiber into red clay. The range of confining pressure was 50–200 kPa; fiber content was 0.1%–0.4%; and fiber length was 10–40 mm. By varying the confining pressure, fiber content and fiber length, the unconsolidated and undrained triaxial tests were used to study the shear strength variation law of coir fiber-reinforced soil. The experimental data were processed to establish a linear model of the segmental elastic modulus, and linear analysis was used to determine the model fitting parameters and to improve the Duncan-Chang model by combining the concept of damage ratio. The modified Duncan-Chang model fits the stress-strain relationship of coir-reinforced soil. The results show a clear dividing line for the effect of fiber length and fiber content on the strength of the samples, which is about 30 mm and 0.3%, respectively. At the same time, the modified model can fit the stress-strain relationship of coir fiber-reinforced soil and reflect the stress-strain curve characteristics of coir fiber-reinforced soil.

KEYWORDS

coir fiber-reinforced soil, strength law, elastic modulus, modified Duncan-Chang model, triaxial test, axial strain

1 Introduction

The ecological environment has always been closely related to human beings. In the field of civil engineering, a series of projects such as urban construction, slope reinforcement, and road planning require necessary soil reinforcement. Finding an ecologically beneficial soil reinforcement technology is significant and has broad application prospects. In recent years, the fiber-reinforced soil method has received more attention and research. Currently, the types of engineering materials are mainly classified as natural and synthetic fibers (Mahdi Hejazi et al., 2012). Natural fibers include plant fibers, mineral fibers, animal fibers, etc., and synthetic fibers contain carbon fibers, glass fibers, metal fibers, etc. Compared to synthetic fibers, natural fibers are not only easy to obtain but also do not require high cost. Coconut shell fiber is a plant fiber, and its price is only 1/20 of carbon fiber. At the same time, coir fiber has high strength, toughness, and renewable properties and is a natural environmental protection material. Fiber-reinforced

red clay soil is a physical way to change the original mechanical properties of the soil (Liu et al., 2013). The use of coir fiber for the reinforcement of red clay soil is still relatively new, and its reinforcement mechanism and strength law need further research.

Currently, scholars have taken various forms of experimental studies on the mechanical properties of fiber-reinforced soils. Three main aspects are involved. The first is which aspects of the reinforcing effect of the soil after the addition of fibers are reflected. Compaction tests on soil samples after adding coir fibers to the soil revealed that the fibers affected physical properties such as maximum dry density and optimum moisture content of the soil (Jairaj et al., 2018). Direct shear tests on fiber-reinforced soils revealed that the soil was less brittle, cohesion increased by about 4.3–8.8 kPa, and internal friction angle increased by about 0.51°–4.36° after fiber addition. The loss of soil strength after reaching its peak is also reduced (Zhang et al., 2001; Yetimoglu and Salbas, 2003; Qin et al., 2017). In addition, adding coir fibers will enhance parameters such as shear strength and modulus of elasticity of the soil. Adding coir fibers to expansive soils increases the strength of soil samples by about 1.1–1.37 times (Sivakumar Babu et al., 2008; Widianti et al., 2021). Thus, what role do the fibers play in the soils? The fibers are combined with soil particles through friction and cohesion, and the fibers can interweave with each other to form a spatial mesh structure that increases the strength of the sample (Zhang et al., 2021). The researchers mentioned above mainly used the method of basic tests to study fiber-reinforced soils and less often used more accurate test protocols to test the fiber-reinforced soils. In this paper, a triaxial apparatus was used to study fiber-reinforced soils. The test results were more accurate, facilitating the study of fiber-reinforced soils using a model-fitting approach. The second one is the effect that the different properties of fiber length and content can have on the soil. The unconfined compressive strength of clay soils increases with increasing fiber content, increasing the compressive strength by about 150% compared to the clay strength (193 kN/m^2) (Kumar et al., 2005). The fiber content strengthens the soil more effectively than the fiber length (Consoli et al., 2007). The longer the fiber length and the more the incorporation at the same perimeter pressure, the better the reinforcement effect of the fiber (Liu et al., 2011). Both the tensile and compressive strength of fiber soil samples increased with time (Anggraini et al., 2015). The above studies only briefly described the relationship between fiber properties and reinforcement effectiveness and did not further explore the specific relationship between the two. For example, whether there is an optimal solution for the reinforcement effect of fiber length and fiber content on the soil will be the focus of the research in this paper. The third one is in the physical model test. Polyester fibers were mixed into the soil to simulate a sloping soil surface layer. The test results showed that the root system simulated by polyester fibers helped to reduce rainwater infiltration, delay the rise of the water table, and improve the soil shear strength (Eab et al., 2014). Using coir fibers to strengthen the foundation can reduce foundation settlement (Lal et al., 2017; Fang et al., 2023). Soils reinforced with vegetation were simulated with a mixture of clay and glass fibers, and the results showed that the deeper the roots, the deeper the sliding surface, with a difference of about twice the depth between the two (Catalina et al., 2022). These studies provide strong support for fiber-reinforced soils in terms of simulating engineering reality, etc., and are instructive for applying fiber-reinforced soils in engineering practice. It is also a direction for further research on coir fiber-reinforced soils.

Researchers have conducted numerous experimental studies on fiber-reinforced soils regarding fiber types, reinforcement effects, foundation simulation tests, and fiber-soil composition forms. However, the focus of the research is only at the level of experimental tests. The strength properties of fiber-reinforced soils have yet to be investigated by combining the test results with relevant theories. The Duncan-Chang model is essentially a linear stiffness softening the law, while the coir fiber-reinforced soil samples show a non-linear stiffness softening. Therefore, this model could be more accurate for describing the intrinsic relationship of non-linear strain softening. Shen and Zhang et al. (1988) proposed a theory of soil damage. According to the stress-strain relationship of the conventional triaxial test, the shear deformation of strong structural clay soil is divided into the undamaged structural stage, structural progressive damage stage, and structural complete damage stage (Zhang et al., 2022). Structural soils vary in their structural yield stresses with test conditions and require constructing a non-linear model of the segmental elastic modulus (Wang, 2006; Yang and Liang, 2014). The damage concept proposed by Shen Zhujiang was applied to the original Duncan-Chang model, and the model was improved. The improved hyperbolic function can simulate the stress-strain relationship of structural clay very well (Wang et al., 2004). Based on the improved Duncan-Chang model, the stress-strain relationship of the original red clay was simulated and calculated. The model could better reflect the development of soil stress-strain at different stages (Gu et al., 2020). These studies above have indicated clear directions for the improvement of the model, and this paper combines the above approaches to revise the model. In the field of fiber-reinforced soils, fewer studies combine with theoretical models. Based on the modified Duncan-Chang model, this paper introduces the stress-strain relationship data of coir fibers, fits the experimental data of fiber-reinforced soil by improving the Duncan-Chang model, and analyzes its strength law to explore the accuracy of the fitting results of the stress-strain curve of fiber-reinforced soil. These results will provide an essential basis for an in-depth understanding of the strength theory of coir fiber-reinforced soils and provide theoretical support for applying coir fiber-reinforced soils in engineering construction.

2 Experimental design

2.1 Test materials

The red clay samples were taken from the Central South University of Forestry and Technology area in Changsha, Hunan province, China. The depth of the red clay samples was 50–70 cm, and the soil was brown-red. According to GB/T50123-2019, the

TABLE 1 Performance parameters of coir fiber.

No.	Length (mm)	Single ultimate tension (kN)	Diameter (mm)	Tensile strength (MPa)	Ten ultimate tension (kN)	Mean diameter (mm)	Tensile strength (MPa)
1	60	5.3	0.23	127.56	55.2	0.23	1328.60
2	60	5.1	0.22	134.16	52.7	0.22	1386.36

FIGURE 1
Coir fiber-reinforced soil with a diameter of 61.9 mm and height of 125 mm.

physical properties of the soil were measured. The natural moisture content of undisturbed soil is 25.66%, the liquid limit is 49.0%, the plastic limit is 22.7%, the plastic index is 26.3, the dry density is 1.47 g/cm^3, the specific gravity is 2.74, the maximum dry density is 1.694 g/cm^3, the optimum moisture content is 20.2%. The performance parameters of coir fiber are shown in Table 1.

2.2 Sample preparation

The sample sizes commonly used in triaxial studies of fiber-reinforced soils are currently of two types, 39.1 and 50 mm in diameter, under restricted test conditions. According to Ang and Erik Loehr (2003), the sample diameter exceeds 70 mm, and the sample is more likely to represent the strength of fiber-reinforced

FIGURE 2
The distribution of coir fiber in the sample.

soil reasonably. Therefore, in order to avoid side effects and to consider the laboratory conditions, the tests in this paper used larger samples than previous sizes to investigate the strong pattern of coir fiber-reinforced soils. The sample diameter is 61.9 mm, and the height is 125 mm, as shown in Figure 1. The preparation process was carried out about the Standard for Geotechnical Test Methods (GB/T50123-2019). According to the calculation results, the prepared coir fibers with different contents were added to the soil particles in proportion to the mix well. It was put into the three-valve membrane, in turn, to compact it, thus forming a new soil structure. The distribution of coir fibers in the sample is shown in Figure 2. The compaction method was used to make the sample, and the control compaction degree was 95% of the maximum dry density. To simulate the pore state of the soil in the actual project, the prepared samples were put into the vacuum saturator (Apparatus No. 21110155LQ, apparatus located in Room 301 of the Civil Engineering Experiment Center). After the saturation was finished, the samples were encapsulated and stored in cling film.

2.3 Test procedure

According to the experimental conditions, the stress-strain relationship of coir fiber-reinforced soil study by the unconsolidated and undrained triaxial shear test method. The

TABLE 2 Test conditions.

No.	Fiber content (%)	Fiber length (mm)	Confining pressure (kPa)
1	0	0	100
2	0.1, 0.2, 0.3, 0.4	30	100
3	0.3	10, 20, 40	100
4	0.3	30	50, 150, 200

experiment was carried out on a Nanjing TKA triaxial tester (Apparatus No. 202001007, apparatus located in Room 301 of the Civil Engineering Experiment Center), which consists of a computer, an axial compression system, a confining pressure system and a pressure chamber. It can automatically control the test process and data acquisition.

The test process is as follows: the coir fiber-reinforced soil sample covered with latex film is placed in the pressure chamber and filled with water. Apply specific confining pressure with a confining pressure system. When the confining pressure reaches a predetermined value, the sample is sheared by a computer-controlled axial compression system at a constant axial loading rate. According to the test code, the shear strain rate was calculated to be 0.625 mm/min. A computer collects and processes the data of axial pressure, deflection stress, and axial deformation during loading. The maximum deviated stress value was used as the damage standard of the sample in the test. Four different circumferential pressures were selected for the tests, 50, 100, 150, and 200, respectively. Fiber content was chosen by mass percentages, 0, 0.1%, 0.2%, 0.3%, and 0.4%, respectively. The fiber lengths were 10, 20, 30, and 40 mm. The test conditions for the specific samples are shown in Table 2.

3 The arrangement and analysis of test data

3.1 Failure mode of coir fiber-reinforced soil

Influenced by the coir fiber, the samples underwent obvious plastic deformation during the test. As shown in Figure 3A, without adding coir fibers, the soil samples showed an obvious diagonal crack during the damage, which exhibited brittle damage; as shown in Figure 3B, after the addition of fibers, the damage showed bulging damage. Although a certain shear surface was also generated, the degree of shear was substantially reduced compared with that without the addition of coir fibers. Therefore, the damaged form of the coir fiber-reinforced soil is a mixture of ductile and brittle damage. This intuitively indicates that coir fiber can reduce the degree of damage to soil samples.

3.2 The variation law of deviating stress and strain

3.2.1 Effect of fiber length

Figure 4 shows the q-ε ($q = \sigma_1 - \sigma_3$, q is deviator stress) stress-strain curve of coir fiber at 100 kPa confining pressure and 0.3% fiber content at different fiber lengths. During the test, it was found that the fiber length over 50 mm is easy to twist into clumps, which will make the sample making more difficult and the strength of the sample is significantly reduced. Therefore, four different fiber lengths of 10, 20, 30, and 40 mm were used in this paper. The values of the deviator stress in the stress-strain relationship curves differed significantly for the samples with different test parameters. When the fiber length increased in the range of 0–30 mm, the deviator stress of the samples gradually increased with the increasing length of fiber. When the fiber length exceeded 30 mm, further increasing the length of coir fiber would not increase the deviator stress. When the fiber length was 40 mm, the deviator stress of the sample at the same axial strain position was lower than that of the 20 mm fiber length. This indicates that the effect of fiber length on the strength of the sample is pronounced, and the excessive fiber length causes the fibers themselves to associate with each other and form a dense web-like structure. This hinders the formation of a composite structure between the soil and the coir fibers, which results in the reinforcing effect of the fibers not being fully developed.

3.2.2 Effect of fiber content

Figure 5 shows the stress-strain curves of different fiber contents under confining pressure of 100 kPa and fiber length of 30 mm. The percentage of fiber mass to soil sample mass was used as the fiber content to investigate the effect of fiber mass on the strength of the samples. When the fiber content reaches 0.5%, the excessive fibers cause them to aggregate with each other, and the produced samples easy form weak zones. Therefore, four different fiber contents of 0.1%, 0.2%, 0.3%, and 0.4% were used. As the fiber content grew from 0% to 0.3%, the deviator stress gradually increased. However, when the fiber content exceeded 0.3%, the deviator stress of the samples started to decrease, and then increasing the amount of coir fiber participation would not improve the strength of the samples.

The content and length of coir fiber affect the strength of coir fiber, but they have different effects. When the fiber content increases to 0.4%, the deviator stress at the same axial strain position is lower than 0.3% fiber content but higher than that at

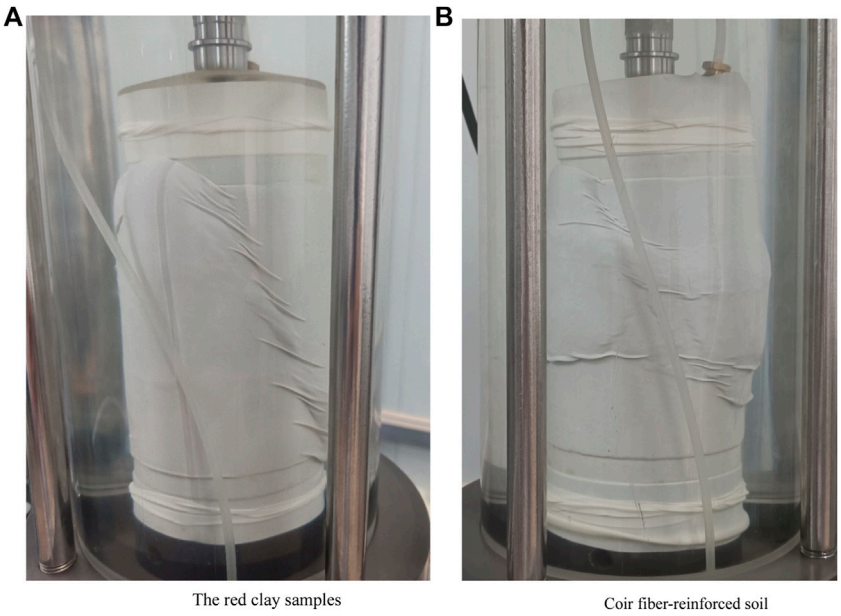

FIGURE 3
Mode of sample failure. **(A)** The red clay samples, **(B)** Coir fiber-reinforced soil.

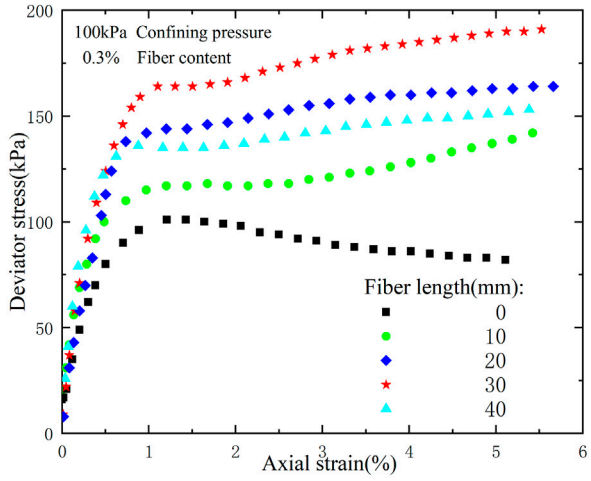

FIGURE 4
Effect of fiber length within 0–40 mm on stress-strain of samples at constant confining pressure and fiber content.

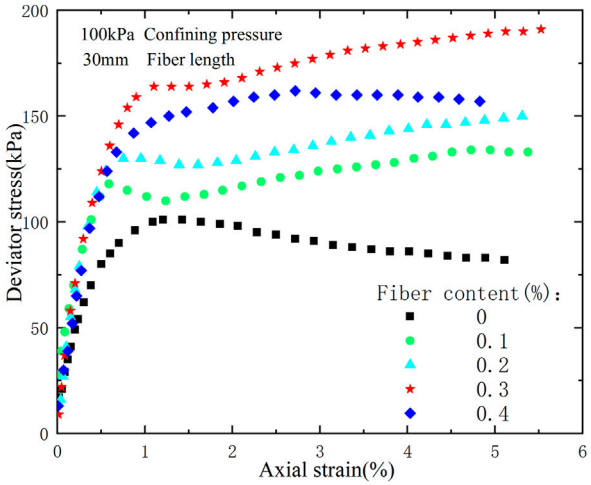

FIGURE 5
Effect on stress-strain of samples at 0%–0.4% of fiber content at constant confining pressure and fiber length.

0.2% fiber content. This indicates that the excessive fiber content will also negatively affect the sample's strength, but the effect is weaker than the fiber length. Too much fiber also leads to fiber binding, which is not conducive to the connection between soil particles and fiber. Therefore, the effect of coir fiber on red clay is equivalent to the effect of reinforced material on cement, and there is an optimal content and length.

Figures 6, 7 show that the strength of the sample changes with increasing fiber length and content. When no fiber is added, the stress-strain relationship is a softening curve. When fibers are added, the stress-strain relationship is a hardening type of curve, and the deviator stress increases with the development of axial strain. The coir fiber has a good anchoring effect. When the fiber action, the value of the

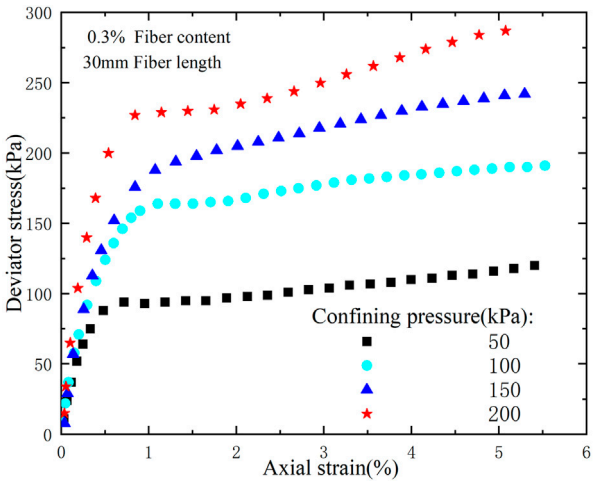

FIGURE 6
Effect of stress-strain on samples within 50–200 kPa of confining pressure with constant fiber length and fiber content.

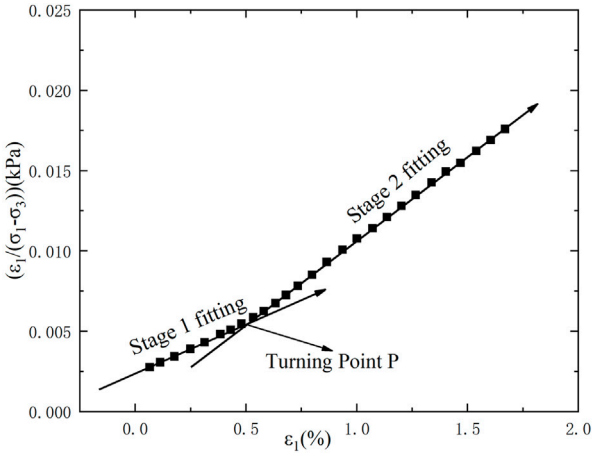

FIGURE 7
Relation between axial strain ratio deviator stress and axial strain.

deviator stress of the sample was significantly larger than the sample without the addition of fiber. When the axial strain did not reach 1.5%, both strengths increased with strain development. With the axial strain's further development, the fibre sample's deviator stress continued to grow. For the samples without added fiber, the value of deviator stress started to decrease, and the difference between the two gradually increased. As the strain grows, the deviator stress's differential value also increases. This indicates that the fibers are becoming more and more effective in reinforcing red clay soils.

3.2.3 Effect of confining pressure

Figure 6 shows the stress-strain curve of samples under different confining pressures with 0.3% coir fiber content. The depth of fiber soil cover in construction engineering is about 0–15 m, and the soil pressure is determined as the product of dry density (1.47 g/cm^3) and gravitational acceleration (9.8 m/s^2) and depth. Therefore, the range of soil pressure is 0–220 kPa, so four levels of 50, 100, 150, and 200 kPa are used to simulate the actual working conditions of the fiber-reinforced soil. With the same fiber length and fiber content, the deviator stress increases with the step-by-step increase of the confining pressure.

3.3 Discussion and analysis

After the above analysis, the strength properties of the fiber-reinforced soil samples exhibited the optimum situation at a fiber length of 30 mm and a fiber content of 0.3%, and their stress-strain curves are shown in Figures 6, 7. The stress-strain curves of the fiber-reinforced soil samples under different test parameters were similar in shape, and all of them retained the essential characteristics of hyperbolic curve. For the fiber-reinforced soil samples, the damage stage is significantly different from that of the red clay soil. After the red clay soil samples reached the damage stage, the stress decreased with the increase of axial strain. In contrast, after the fiber-reinforced soil reached the damage stage, the stress continued to increase with the growth of axial strain, and the damage form showed a hardening characteristic. After the addition of fibers to the soil, the combination of the two forms a new structure. The incorporation of fibers has a significant impact on the mechanical properties of the sample. Soil particles in contact with fibers form a new arrangement. Their structural composition is changed, manifested by a decrease in density and compaction, and a substantial increase in plastic deformation capabilities. The stress-strain characteristics are as follows: when the plastic deformation is small, the stress-strain curve rises faster, or the stress increase is more prominent. When the plastic deformation is larger, the deviator stress of some samples appears to fall and then increase. With the further growth of strain, the stress-strain curve gradually tends to flatten out, and the deviator stress will keep growing slowly. Therefore, adding fiber can effectively limit the deformation of the soil, improve the soil's strength index, and effectively change the soil's original stress-strain field, thus optimizing the engineering performance of the soil.

4 A modified Duncan-Chang model of coir fiber-reinforced soil

4.1 Modified Duncan-Chang model

The structural damage law promoted by Shen and Zhang (1998) regards the structural state of soil as two different forms: the non-damaged state and the remodeled state. The soil body is

in a combination of both the non-damaged state and the remodeled state when the force deforms it, and with the gradual increase of the load, the state in which the soil sample is in can be expressed by the formula

$$S = (1 - \omega)S_i + \omega S_d \quad (1)$$

In the formula: S is the mechanical parameter of the soil; S_i is the strength property of the soil in the lossless state; S_d is the strength property of the soil in the remodeled state; ω is the damage ratio, the proportion of the soil in the remodeled state to the whole soil.

Eq. 1 is brought into the Duncan-Chang model to derive the modified hyperbolic function

$$\frac{\varepsilon_1}{(\sigma_1 - \sigma_3)} = a_m + b_n\varepsilon_1 \quad (2)$$

In the formula: $a_m = \frac{1}{(1-\omega)E_{i1}+\omega E_{i2}}$; $b_n = \frac{1}{(1-\omega)(\sigma 1-\sigma 3)_{u1}+\omega(\sigma 1-\sigma 3)_{u2}}$; $\omega = 1 - e^{-\frac{\varepsilon_1}{\varepsilon_{1u}-\varepsilon_1}}$; E_{i1} and E_{i2} are the elastic modulus of the first and second stages, respectively; $(\sigma_1\text{-}\sigma_3)_{ult1}$ and $(\sigma_1\text{-}\sigma_3)_{ult2}$ are the deviator stress limit values of the fitted straight lines of the first and second stages, respectively; ω is the damage ratio; ε_{1u} is the axial strain corresponding to the soil body at the time of damage.

By analyzing the triaxial test data, the undamaged structural stage and the structural gradually damaged stage of the reinforced soil sample are regarded as the first stage of strength deformation; then the structural completely damaged stage is made the second stage of strength deformation.

In Figure 7, the stress-strain relationship curve $\varepsilon_1/(\sigma_1\text{-}\sigma_3) \sim \varepsilon_1$ consists of two stages, ε_1 is at 0%–0.5% and ε_1 is greater than 0.5% after. Two straight lines can be fitted to these two stages respectively. Since the yield stress state of the soil changes with the change in loading conditions. As the stress changes, the sample gradually produces damage, and when the stress changes to a large enough, the damage will be more obvious, which is shown as the appearance of a turning point on the $\varepsilon_1/(\sigma_1\text{-}\sigma_3) \sim \varepsilon_1$ curve, and this turning point is regarded as the turning point of the two straight lines of the first and second stages. The turning point's appearance indicates that the sample's damage has developed from the first stage to the second stage, and its elastic modulus and ultimate deviator stress will also change significantly, which is presented in the coordinate system in Figure 7 as the change of intercept and slope.

As shown in Figure 7, each stage can be fitted linearly, and the corner mark k refers to two different steps in the hardening process. The formula is expressed as

$$y = a_k + b_k x \,(\mathrm{k} = 1, 2) \quad (3)$$

The asymptotic values of elastic modulus and deviator stress at each stage are obtained from the following equations.

$$E_{ik} = 1/a_k \,(k = 1, 2) \quad (4)$$

$$(\sigma 1 - \sigma 3)_{ultk} = 1/b_k \,(k = 1, 2) \quad (5)$$

4.2 Modified Duncan-Chang model parameter solution

In this paper, the stress-strain curve of coir fiber-reinforced soil is fitted using the hyperbolic function of Eq. 2. First, a part of the data with abnormal values will appear at the beginning of the test. After removing these anomalous data, the relationship image of $\varepsilon_1/(\sigma_1\text{-}\sigma_3)\sim\varepsilon_1$ was plotted by data processing software. The stress-strain relationship is shown in Figure 7, and there are two obvious phases in the image. Point P is the turning point. A straight-line fit was performed for each of the two phases, and the fit was above 97%. Then, the values of parameters E_{i1}, E_{i2}, $(\sigma_1\text{-}\sigma_3)_{ult1}$, and $(\sigma_1\text{-}\sigma_3)_{ult2}$ are determined according to the Eqs 3–5. The same method was adopted to fit the data of each sample into a straight line to find out the values of the above four parameters. The calculated parameters are shown in Table 3.

The elastic modulus of stage 1 and stage 2 are shown in Table 3, showing the relationship between elastic moduli and fiber content, fiber length, and confining pressure under different test parameters. With the increase in fiber content and length, the elastic modulus of coir fiber-reinforced soil shows a trend of increasing first and then decreasing. The elastic modulus reaches the maximum value when the fiber content and length reach 0.3% and 30 mm, respectively. If the fiber content and length continue to increase, the elastic modulus decreases, and the ability to resist deformation of the sample decreases. For the same fiber content and length, the higher the confining pressure, the greater the elastic modulus. That is, the higher the resistance to deformation.

The values of ultimate deviator stress in stage 1 and stage 2 are shown in Table 3, showing the relationship between ultimate deviator stress and fiber content, fiber length, and confining pressure under different test parameters. The ultimate deviator stress value variation gradually increases when the fiber content is from 0.1% to 0.3%. Similarly, the ultimate deviator stress increases gradually when the fiber length is 10–30 mm. As the fiber content and fiber length continue to grow, the strength of the sample begins to decrease after reaching the optimum content and optimum length. The relationship between the modulus of elasticity and the confining pressure is shown by the fact that for the same sample with the same fiber content and fiber length, the value of the ultimate deviator stress increases with increasing confining pressure, and the sample exhibits higher strength. As can be seen from Table 3, the values of ultimate deviator stress $(\sigma_1\text{-}\sigma_3)_{ult1}$ for the same group of samples are all higher than $(\sigma_1\text{-}\sigma_3)_{ult2}$, indicating that the samples reinforced with coir fiber are suitable for modified Duncan-Chang model.

Based on the model and the pattern exhibited by the experimental results, the sample deviator stress also increases when the fiber content increases from 0.1% to 0.3%. When the fiber content was 0.4%, the sample deviator stress still kept

TABLE 3 Stress-strain calculation parameters of coir fiber-reinforced soil.

Model parameters	Fiber content/%					Fiber length/mm				Confining pressure/kPa			
	0	0.1	0.2	0.3	0.4	10	20	30	40	50	100	150	200
$10^3/E_{i1}$	2.6	2.5	2.0	1.9	2.0	2.8	2.3	1.9	2.3	2.2	1.9	1.7	1.4
$10^3/(\sigma_1-\sigma_3)_{ult1}$	7.1	4.5	4.9	4.0	4.3	5.3	4.2	4.0	5.1	5.2	4.0	3.6	2.8
$10^3/E_{i2}$	2.2	1.3	1.2	1.1	1.3	2.1	1.9	1.1	1.6	1.7	1.1	1.0	0.8
$10^3/(\sigma_1-\sigma_3)_{ult2}$	11.8	7.8	6.9	5.8	6.5	6.2	5.7	5.8	6.2	7.1	5.8	4.5	3.7

increasing, but the value was less than 0.3% of fiber content. It indicates that the fiber content significantly changes the reinforcement effect of red clay samples at 0.3%. Similarly, based on the test conditions and experimental results, it can be concluded that the fiber length is optimal when it reaches 30 mm.

5 Discussion of the model fitting results

The experimental results and the fitted results are plotted on the same coordinate axes as in Figure 8. The experimental data of the coir fiber-reinforced soil samples were consistent with the fitted data of the improved model. In the case of small strains (ε_1 < 1%), the fitted results are slightly larger compared to the measured values, but there is no significant deviation in general. The use of the modified model to fit the coir fiber-reinforced soil has the following advantages: its variation law is consistent with the actual situation, and the parameters of the modified model are obtained in a simple and clear sense, which provides theoretical guidance for the study of the strength law of coir fiber-reinforced soil.

In order to explore the accuracy of the modified Duncan-Chang model in fitting the remaining coir fiber-reinforced soil samples, the test data of several groups of samples were fitted. The fit results are shown in Figures 9–11.

In the axial deformation at about 1%, the fitted curve of the sample is higher than the curve drawn from the test data. The reason is that this part is in the junction area between the first and second stages of the $\varepsilon_1/(\sigma_1-\sigma_3)$~$\varepsilon_1$ curve, and this area contains the turning point of the two fitted straight lines in the modified model, which leads to a change in the values of the model parameters in this part, thus causing a difference between the fitted curve and the experimental data here. When the deformation of the sample develops from the first stage to the second stage, the solution of the fitted data changes from a straight line in the first stage to a straight line in the second stage. At this time, the intercept of the line becomes smaller and the slope increases. The modulus of elasticity increases while the ultimate deviator stress decreases. For the second stage, the fit between the model fitting curve and the test data curve is higher in the case of larger axial strain.

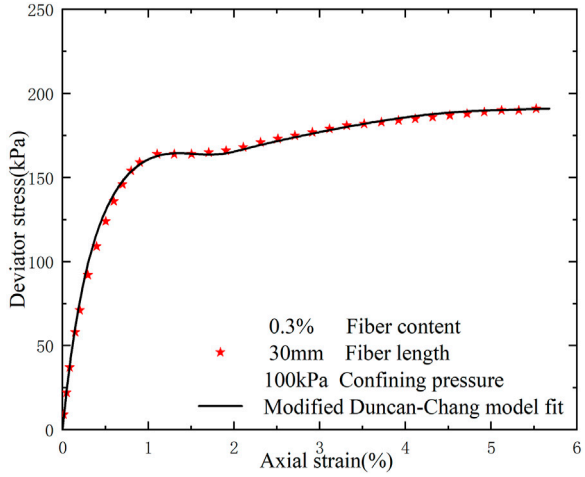

FIGURE 8
Comparison of data at 0.3% fiber content with model fitting results.

6 Conclusion

In this paper, larger triaxial samples are used. The experimental demonstration and model validation are provided for studying the strong law of coir fiber-reinforced soil by comparing the experimental data with the fitted curve of the modified Duncan-Chang model. At the same time, it provides a significant reference value for the strength theory research of coir fiber-reinforced soil. The following conclusions were drawn:

(1) At the beginning of loading, the eccentric stress increases rapidly when the axial strain is minor. With the increase of the axial strain, the curve tends to be smooth. The comparison of coir fiber-reinforced soil and red clay

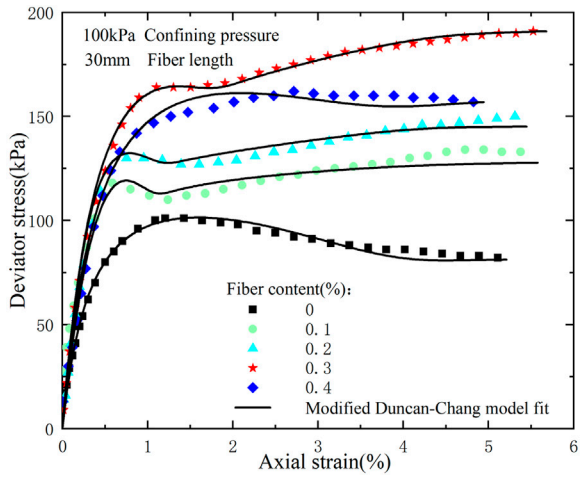

FIGURE 9
Comparison of data with model fitting results for fiber content 0%–0.4%.

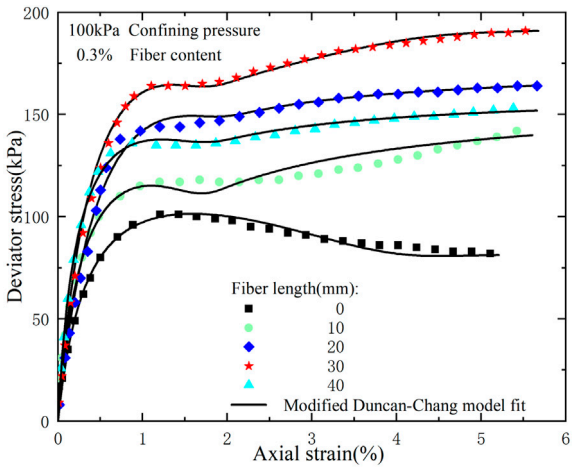

FIGURE 11
Comparison of model fitting results for fiber length 0–40 mm.

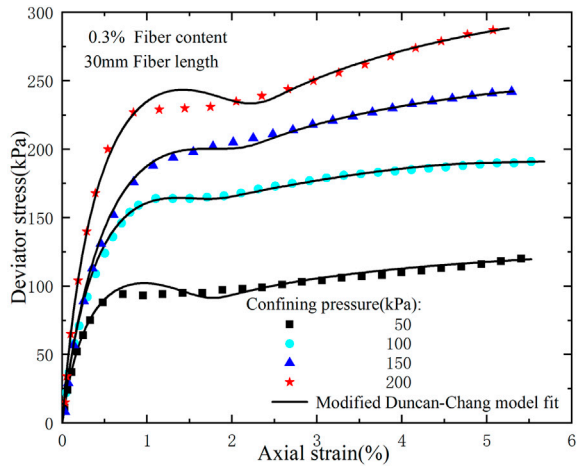

FIGURE 10
Comparison of model fitting results for confining pressure 50–200 kPa.

shows that the difference in deviator stress of different samples gradually increases, and the effect of coir fiber-reinforced soil is remarkable.

(2) The ultimate deviating stress and elastic modulus increase and then decrease with the increase of coir fiber content and length. The effect of fiber length and fiber content on the strength of coir fiber-reinforced soil has an obvious boundary, the cut-off length and the amount of doping are about 30 mm and 0.3%, respectively. When it is below this limit, the elastic modulus and ultimate deviator stress of coir fiber-reinforced soil increase with the increase of fiber length and fiber content, and when it is above this limit, they begin to decrease.

(3) Under the condition of the same fiber length and content, the strength of coir fiber-reinforced soil under the same axial strain increases with the increase of confining pressure step by step. That is to say, the greater the confining pressure, the higher the sample's strength.

(4) From the point of view of structural damage, the stress-strain relationship of coir fiber-reinforced soil was divided into two stages, which the modified Duncan-Chang model fitted.

(5) The calculation of the formula obtains the exact parameters of the fit model. The modified Duncan-Chang model can fit the stress-strain relationship of coir fiber-reinforced soil, and the fit degree is high.

Data availability statement

The original contributions presented in the study are included in the article/Supplementary Material, further inquiries can be directed to the corresponding author.

Author contributions

Performed research, analyzed data, and wrote the paper, PL; designed research and revisions, HY; designed research and revisions, XJ; analyzed data, EY; analyzed data, JC.

Funding

Five projects supported the study, which are the National Natural Science Foundation of China (31971727), the Science and Technology Innovation Program of Hunan Province (Grant No.: 2022NK2056), the Forest Science and Technology Innovation Program of Hunan Province (XLK202105-3), the Special Fund Project of Safety Production Prevention and Emergency Response of Hunan Province in 2021 (Grant No.: 2021-QYC-10008-24956) and the Hunan Provincial Natural Science Foundation Project (Grant No.: 2022JJ31005).

Acknowledgments

The authors are very grateful to the editor and reviewers for their valuable advice.

Conflict of interest

The authors declare that the research was conducted in the absence of any commercial or financial relationships that could be construed as a potential conflict of interest.

Publisher's note

All claims expressed in this article are solely those of the authors and do not necessarily represent those of their affiliated organizations, or those of the publisher, the editors and the reviewers. Any product that may be evaluated in this article, or claim that may be made by its manufacturer, is not guaranteed or endorsed by the publisher.

References

Ang, E. C., and Erik Loehr, J. (2003). Sample size effects for fiber-reinforced silty clay in unconfined compression[J]. *Geotechnical Test. J.* 26 (2), 191–200. doi:10.1520/GTJ11320J

Anggraini, V., Asadi, A., Huat, B. B. K., and Nahazanan, H. (2015). Effects of coir fibers on tensile and compressive strength of lime treated soft soil. *Measurement* 59, 372–381. doi:10.1016/j.measurement.2014.09.059

Catalina, L., Mendoza, C., and Jose Vicente, A. (2022). Physical and numerical modeling of clayey slopes reinforced with roots[J]. *Int. J. Civ. Eng.* 20 (9), 1115–1128. doi:10.1007/S40999-022-00733-0

Consoli, N. C., Casagrande, M. D. T., and Coop, M. R. (2007). Performance of a fibre-reinforced sand at large shear strains. *Géotechnique* 57, 751–756. doi:10.1680/geot.2007.57.9.751

Eab, K. H., Takahashi, A., and Likitlersuang, S. (2014). Centrifuge modelling of root-reinforced soil slope subjected to rainfall infiltration. *Géotechnique Lett.* 4 (3), 211–216. doi:10.1680/geolett.14.00029

Fang, K., Tang, H., Li, C., Su, X., An, P., and Sun, S. (2023). Centrifuge modelling of landslides and landslide hazard mitigation: A review. *Geosci. Front.* 14 (1), 101493. ISSN 1674-9871. doi:10.1016/j.gsf.2022.101493

Gu, J., Fan, L., Lu, H., and Chen, Y. (2020). Simulation of the stress-strain relationship of red clay based on the modified Duncan-Chang model [J]. *J. Guilin Univ. Technol.* 40 (02), 351–357. doi:10.3969/j.issn.1674-9057.2020.02.013

Jairaj, C., Prathap Kumar, M. T., and Raghunandan, M. E. (2018). Compaction characteristics and strength of BC soil reinforced with untreated and treated coir fibers. *Innov. Infrastruct. Solut.* 3 (1), 21. doi:10.1007/s41062-017-0123-2

Kumar, A., Singh Walia, B., and Mohan, J. (2005). Compressive strength of fiber reinforced highly compressible clay. *Constr. Build. Mater.* 20 (10), 1063–1068. doi:10.1016/j.conbuildmat.2005.02.027

Lal, D., Sankar, N., and Chandrakaran, S. (2017). Effect of reinforcement form on the behaviour of coir geotextile reinforced sand beds. *Soils Found.* 57 (2), 227–236. doi:10.1016/j.sandf.2016.12.001

Liu, B., Tang, C., and Jian, L. (2013). etc. Research progress on engineering properties of fiber-reinforced soil. *J. Eng. Geol.*, 540–547. doi:10.3969/J.ISSN.1004-9665.2013.04.009

Liu, F., Sun, H., and Xiurun, G. (2011). Triaxial test study on glass fiber-reinforced soil [J]. *J. Shanghai Jiao Tong Univ.* 45 (05), 762–766+771. doi:10.16183/J.CNKI.JSJTU.2011.05.028

Mahdi Hejazi, S., Sheikhzadeh, M., Abtahi, S. M., and Ali, Z. (2012). A simple review of soil reinforcement by using natural and synthetic fibers. *Constr. Build. Mater.* 30, 100–116. doi:10.1016/j.conbuildmat.2011.11.045

Qin, W., Li, G., Hu, W., Li, B., and Zou, G. (2017). Triaxial test study on Coir soil [J]. *Sci. Technol. Eng.* 17 (10), 272–276. doi:10.3969/j.issn.1671-1815.2017.10.047

Shen, Z., and Zhang, W. (1988). "Applying damage mechanics to soil mechanics [C]," in 3rd Proceedings of the National Symposium on Numerical Analysis and analytical methods of geotechnical mechanics, 595–609.

Sivakumar Babu, G. L., Vasudevan, A. K., and Sayida, M. K. (2008). Use of coir fibers for improving the engineering properties of expansive soils. *J. Nat. Fibers* 5 (1), 61–75. doi:10.1080/15440470801901522

Wang, L. Z., Zhao, C. Y., and Li, L. L. (2004). A modified Duncan-Zhang model considering soil structural properties [J]. *J. Water Resour.* (01), 83–89. doi:10.3321/j.issn:0559-9350.2004.01.016

Wang, W. (2006). Study on piecewise tangent modulus of nonlinear soil model [J]. *J. Hohai Univ. Sci.* (02), 204–207.

Widianti, A., Diana, W., and Alghifari, M. R. (2021). Shear strength and elastic modulus behavior of coconut fiber-reinforced expansive soil. *IOP Conf. Ser. Mat. Sci. Eng.* 1144 (1), 012043. doi:10.1088/1757-899x/1144/1/012043

Yang, A., and Liang, C. (2014). Study on the stress-strain relationship of soft structural soil based on Duncan-Chang model [J]. *Hydrogeology Eng. Geol.* 41 (04), 75–79+86. doi:10.16030/J.CNKI.ISSN.1000-3665.2014.04.012

Yetimoglu, T., and Salbas, O. (2003). A study on shear strength of sands reinforced with randomly distributed discrete fibers. *Geotext. Geomembranes* 21 (2), 103–110. doi:10.1016/s0266-1144(03)00003-7

Zhang, H., Li, H., Li, H., Jin, L., Hu, T., Zhang, H., et al. (2021). Experimental study on strength characteristics of palm fiber-reinforced soil [J]. *Mineral. Explor.* 12 (05), 1264–1271. doi:10.3969/j.issn.1674-7801.2021.05.020

Zhang, X., Zhan, Y., and Zhang, Y. (2001). Experimental study on strength characteristics of fibrous soil [J]. *Roadbed Eng.* (01), 36–38. doi:10.3969/j.issn.1003-8825.2001.01.012

Zhang, Q-M., Pei, L., Yue, G., and Yang, X. (2022). A modified Duncan-Chang model for strongly structural clays [J]. *J. Water Conservancy Water Transp. Eng.* (02), 117–125. doi:10.12170/20210617003